Modal Analysis: the International Journal of Analytical and Experimental Modal Analysis v 8 n 1 Jan 1993 p 63-78

[redacted]

by C.W.Wong, Y.Q.Ni and J.M.Ko, Hong Kong Polytechnic

ABSTRACT

In a previous paper [1], a mathematical model of a nonlinear hysteretic vibration isolator, with amplitude-dependent parameters, was established based on experimental study. In this paper, the corresponding multi-harmonic steady-state response analysis is addressed. The computational method is based on the Galerkin/ Levenberg-Marquardt approach, in which the frequency/ time domain alternation and FFT procedures, as well as numerical search in the transformed time domain, are introduced. The response features of this hysteretic model are identified. Then, the steady-state responses of base-isolated structures are analyzed by the proposed method with the use of modal partial decoupling. Analytical responses of a vibration-isolated frame are compared favorably with experimental findings.

List of Symbols

a_j	fourier coefficients related to cosine terms
a_j^*	fourier coefficients related to sine terms
A	displacement amplitude
A_g	acceleration amplitude of ground excitation
$\{a\}$	vector of displacement harmonic components
c	viscous damping factor
$[C]$	viscous damping matrix
F	external periodic excitation
F_0	exciting force amplitude
f_i	natural frequency for ith mode
$\{f\}$	vector of exciting force harmonic components
$\{g\}$	vector of ground acceleration harmonic components
$[I]$	identity matrix
$[J]$	Jacobian matrix
k	linear stiffness
$[K]$	linear stiffness matrix
m	mass
$[M]$	mass matrix
p_i	participating factor of ith mode
Q	restoring force of hysteretic component
$\{q\}$	vector of hysteretic restoring force harmonic components
$\{r\}$	vector of objective functions
T	period
t	time
$[U]$	mode shape matrix
$\{u_i\}$	vector of ith mode shape
x, x', x''	displacement, velocity and acceleration

Dr.C.W.Wong,Senior Lecturer, Department of Civil and Structural Engineering, Hong Kong Polytechnic,Kowloon,Hong Kong. Y.Q.Ni,Research Assistant, Hangzhou Architectural and Civil Engineering Institute, Hangzhou, China. Dr.J.M.Ko, Principal Lecturer, Department of Civil and Structural Engineering, Hong Kong Polytechnic, Kowloon, Hong Kong.

Final manuscript received: July 7, 1992

$\dot{x}, \ddot{x}$ generalized velocity and acceleration

$\{x\}, \{x'\}, \{x''\}$ vectors of relative displacement, velocity and acceleration

$\{y\}$ vector of modal coordinates

$\{0\}$ null vector

$\{1\}$ unit vector

Greek

λ_k Levenberg-Marquardt parameter

ξ_i viscous damping ratio of ith mode

τ dimensionless time

ω circular frequency of excitation

ω_i circular natural frequency for ith mode

1. Introduction

Nonlinear vibration isolation techniques have developed rapidly in the past decade. The identification and modelling of nonlinear vibration isolation systems, as well as the dynamic response analysis of these systems, are two main aspects of the investigation.

Steady-state dynamic analysis methods of nonlinear systems have been widely investigated in recent years. The incremental harmonic balance (IHB) method, a multi-harmonic frequency domain procedure proposed by Lau et al [2], has been successfully and extensively applied to the steady-state response analysis of nonlinear dynamic systems and related problems [3-7]. The IHB method is a combination of the Newton-Raphson incremental procedure and the harmonic balance (Galerkin) approach. This method deals well with strongly nonlinear systems subjected to arbitrary periodic excitation and is ideally suited to parametric studies. Another frequency domain solution technique accommodating multiple harmonics, is the Galerkin/Newton-Raphson (GNR) method developed by Ferri et al [8-10]. The GNR method and IHB method are equivalent in essence. In the IHB method, the Newton-Raphson procedure is first applied to form a system of linearized incremental equations and the Galerkin procedure is then adopted to obtain incremental solutions. In the GNR method, the first step is the implementation of the Galerkin procedure to result in a set of nonlinear algebraic equations and then the Newton- Raphson solution method is used to solve them iteratively. Both of these two basically equivalent methods have their own advantages and may be alternatively adopted according to actual circumstances. It is worth mentioning that a fast Galerkin (FG) method developed by Ling et al [11] introduces the fast Fourier transform (FFT) to reduce the amount of computational work required to obtain the higher harmonic terms. This procedure may make the implementation of the IHB method and GNR method more efficient. Recently, Cameron et al [12] presented an alternating frequency/ time (AFT) method for the steady-state response analysis of nonlinear systems. The AFT method provides an iterative implementation in the frequency domain, but at each iteration it needs to transform from the frequency domain to the time domain and then switch back, in order to evaluate some nonlinear terms which cannot be analytically expressed in the frequency domain. This procedure shows that information alternation between the frequency and time domains is essential for analyzing steady-state response of some nonlinear systems which may be difficult to obtain only in the frequency domain.

The nonlinear hysteretic vibration isolators, e. g. , lead rubber isolators and wire-cable isolators, have been getting more and more engineering applications owing to their good dry friction damping performance. However, the restoring force of a hysteretic vibration isolator depends not only on the instantaneous deformation but also on the past history of deformation. This hereditary characteristic makes it difficult to accurately describe the dynamic performance of hysteretic vibration isolators.

A simple mathematical model of a nonlinear hysteretic vibration isolator, with amplitude-dependent parameters, has been established [1] based on the trace method [13,14]. In this mathematical model the hysteretic restoring force is explicitly expressed as a function of displacement and velocity only, but the coefficients of the function themselves are continuous functions of a non-independent intermediate

variable –time domain displacement amplitude. Since the displacement amplitude cannot be analytically expressed in terms of displacement response and cannot be transformed directly into the frequency domain according to the assumed displacement harmonic components, it is difficult to form and solve the linearized incremental equations in the frequency domain when the IHB method is applied. In the present paper, a Galerkin method followed by an efficient Levenberg-Marquardt (LM) procedure has been proposed for analyzing the steady-state oscillation of nonlinear hysteretic systems by adopting the above hysteretic model, in which the frequency domain information of the displacement amplitude intermediate variable is acquired by transforming to the time domain and then back by means of the frequency/time domain alternation similar to the AFT method. The displacement amplitude for the time domain is obtained by a numerical search within a time period and a finite-difference approximation to the Jacobian is adopted. The information alternation between the frequency and time domains at each iteration is implemented by FFT.

The response features of the hysteretic model are first identified by the evaluation of frequency response curves. Then, the steady-state responses of base-isolated structures are analyzed by the proposed method with the use of modal partial decoupling. The solution procedure is greatly facilitated when the linear modal coordinates of the structures are introduced and are partially decoupled.

2. Method of Analysis

(a) Governing Equation of Motion

Without losing generality, a single degree of freedom system with a nonlinear hysteretic component under forced periodic excitation is considered. The governing equation of motion of the system can be written as

$$m \cdot x'' + c \cdot x' + k \cdot x + Q(x, x', A, \omega) = F(\omega, t) \tag{1}$$

where $' = \frac{d}{dt}$ and m, c, k are the mass, viscous damping and linear stiffness of system, respectively. $F(\omega,t)$ is the external periodic excitation with period $T = 2\pi/\omega$. $Q(x, x', A, \omega)$ is the restoring force of the nonlinear hysteretic component connected with the system and A is the displacement response amplitude in the time domain. The expression of $Q(x, x', A, \omega)$ has been reached in Ref. [1] as

$$Q(x, x', A\omega) = k_1(A) \cdot x + k_2(A) \cdot x^3 + k_3(A) \cdot x^5 + C(A, \omega) \cdot x' \tag{2}$$

Introducing the dimensionless time $\tau = \omega t$, Eqs. (1) and (2) become

$$m \cdot \omega^2 \ddot{x} + c \cdot \omega \dot{x} + k \cdot x + Q(x, \dot{x}, A, \tau) = F(\tau) \tag{3}$$

and

$$Q(x, \dot{x}, A, \tau) = k_1(A) \cdot x + k_2(A) \cdot x^3 + k_3(A) \cdot x^5 + C(A) \cdot \dot{x} \tag{4}$$

where $' = \frac{d}{d\tau}$, and $k_1(A)$, $k_2(A)$, $k_3(A)$, $c(A)$ are explicit functions of A. The displacement amplitude A is defined as

(5a)

$$A = \max_{t\in[0,T]}|x(t)| = \max_{\tau\in[0,2\pi]}|x(\tau)| \tag{5a}$$

or

$$\begin{aligned} A &= \left[\max_{t\in[0,T]}\{x(t)\} - \min_{t\in[0,T]}\{x(t)\}\right]/2 \\ &= \left[\max_{\tau\in[0,2\pi]}\{x(\tau)\} - \min_{\tau\in[0,2\pi]}\{x(\tau)\}\right]/2 \end{aligned} \tag{5b}$$

(b) The Galerkin Method

The Galerkin method is first applied to the system described by Eq. (3). For steady-state response analysis, an approximate, periodic with period 2π, multi-harmonic solution is assumed

$$x(\tau) \cong \tilde{x}(\tau) = \frac{a_0}{2} + \sum_{j=1}^{N} a_j \cos j\tau + \sum_{j=1}^{N} a_j^* \sin j\tau \tag{6}$$

where N is the number of harmonic terms taken into account, and

$$\{a\} = \left\{a_0 a_1 a_2 \ldots a_N a_1^* a_2^* \ldots a_N^*\right\}^T \tag{7}$$

is the unknown vector containing the first N harmonic components of $x(\tau)$. Substituting Eq. (6) into Eq. (3) and using the Galerkin procedure provides

$$\int_0^{2\pi}\left[m\cdot\omega^2\ddot{\tilde{x}} + c\cdot\omega\dot{\tilde{x}} + k\cdot\tilde{x} + Q\left(\tilde{x},\dot{\tilde{x}},\tilde{A},\tau\right) - F(\tau)\right]\begin{Bmatrix} 1 \\ \cos\tau \\ \cos 2\tau \\ \vdots \\ \cos N\tau \\ \sin\tau \\ \sin 2\tau \\ \vdots \\ \sin N\tau \end{Bmatrix} d\tau = \{0\} \tag{8}$$

Invoking orthogonality has

$$k\cdot a_0 - f_0 + q_0\{a\} = 0 \tag{9a}$$

$$\left(k - m\cdot\omega^2 j^2\right)\cdot a_j + c\cdot\omega j\cdot a_j^* - f_j + q_j\left(\{a\}\right) = 0 \qquad (j = 1,2,\ldots,N) \tag{9b}$$

$$-c\cdot\omega j\cdot a_j+\left(k-m\cdot\omega^2 j^2\right)\cdot a_j^*-f_j^*+q_j^*(\{a\})=0 \qquad (j=1,2,\ldots,N) \tag{9c}$$

where $\{f\}=\left\{f_0 f_1 f_2\ldots f_N f_1^* f_2^*\ldots f_N^*\right\}^T$ is the known harmonic components vector of external periodic excitation $F(\tau)$. The vector $\{q\}=\{q(\{a\})\}=\left\{q_0 q_1 q_2\ldots q_N q_1^* q_2^*\ldots q_N^*\right\}^T$ comprises the Fourier expansion coefficients of the restoring force $Q\left(\tilde{x},\dot{\tilde{x}},\tilde{A},\tau\right)$ corresponding to the displacement harmonic vector $\{a\}$. $\{q\}$ cannot be expressed in terms of $\{a\}$ in closed-form.

(c) The Levenberg-Marquardt Procedure

Eqs. (9a) to (9c) compose a system of $(2N+1)$ order nonlinear algebraic equations with respect to the unknown vector $\{a\}$, in which only the vector $\{q\}$ is nonlinear and is the implicit function of $\{a\}$. For simplicity, Eqs. (9a) to (9c) are denoted as

$$\{r(\{a\})\}=\{0\} \tag{10}$$

An efficient procedure to solve the nonlinear algebraic equations is the Levenberg-Marquardt (LM) algorithm. When it is applied to Eq. (10), the iteration formula is

$$\left\{a^{(k+1)}\right\}=\left\{a^{(k)}\right\}-\left\{\left[J\left(\left\{a^{(k)}\right\}\right)\right]^T\cdot\left[[J]\left(\left\{a^{(k)}\right\}\right)\right]+\lambda_k\cdot[I]\right\}^{-1}\cdot[J]\left\{a^{(k)}\right\}^T\cdot\{r\}\left\{a^{(k)}\right\} \tag{11}$$

where the Jacobian matrix $[J(\{a^{(k)}\})]=\partial\{r(\{a^{(k)}\})\}/\partial(\{a^{(k)}\})$, λ_k is the Levenberg- Marquardt parameter and $|I|$ is the identity matrix.

At each iteration, the objective function vector $\{r(\{a^{(k)}\})\}$ and the Jacobian matrix $[J(\{a^{(k)}\})]$ should be recalculated with updated values of $\{a^{(k)}\}$. But, with a given $\{a^{(k)}\}$, the corresponding $\{q(\{a^{(k)}\})\}$ cannot be directly evaluated from Eq. (4) within the frequency domain. Here, an alternation scheme between the frequency and time domains by FFT and a numerical search within the time domain are introduced to evaluate the values of $\{q(\{a\})\}$ when $\{a\}=\{a^{(k)}\}$. The vector $\{q(\{a\})\}$ is known to be the Fourier expansion coefficients of the restoring force $Q\left(\tilde{x},\dot{\tilde{x}},\tilde{A},\tau\right)$. For a given $\{a^{(k)}\}$, the inverse FFT is implemented for $\{a^{(k)}\}$ to obtain the time domain discrete values of $\tilde{x}(\tau)$ and $\dot{\tilde{x}}(\tau)$ within a period, and the numerical search to these discrete values within the period reveals the displacement amplitude $A\{a^{(k)}\}$. Then the time domain discrete values of the restoring force $Q\left(\tilde{x},\dot{\tilde{x}},\tilde{A},\tau\right)$ within a period, corresponding to $\{a\}=\{a^{(k)}\}$, are evaluated from Eq. (4). By the forward FFT for these time domain discrete values of $Q\left(\tilde{x},\dot{\tilde{x}},\tilde{A},\tau\right)$, the values of $\{q(\{a^{(k)}\})\}$ are acquired.

Similarly, the Jacobian matrix $\partial\{q(\{a^{(k)}\})\}/\partial\{a\}$ is known to be the Fourier expansion coefficients of the partial differential $\partial Q\left(\tilde{x},\dot{\tilde{x}},\tilde{A},\tau\right)/\partial\{a\}$. Although $Q\left(\tilde{x},\dot{\tilde{x}},\tilde{A},\tau\right)$ is only an implicit function with respect to $\{a\}$, $\partial Q\left(\tilde{x},\dot{\tilde{x}},\tilde{A},\tau\right)/\partial\{a\}\Big|_{\{a\}=\left\{a^{(k)}\right\}}$ can still be numerically evaluated by transformation to the time

domain. From Eq. (4), we have

$$\frac{\partial Q\left(\tilde{x},\dot{\tilde{x}},\tilde{A},\tau\right)}{\partial\{a\}}=\frac{\partial Q}{\partial\tilde{x}}\cdot\frac{\partial\tilde{x}}{\partial\{a\}}+\frac{\partial Q}{\partial\dot{\tilde{x}}}\cdot\frac{\partial\dot{\tilde{x}}}{\partial\{a\}}+\frac{\partial Q}{\partial\tilde{A}}\cdot\frac{\partial\tilde{A}}{\partial\{a\}} \tag{12}$$

in which $\partial Q/\partial\tilde{x}$, $\partial Q/\partial\dot{\tilde{x}}$, $\partial Q/\partial\tilde{A}$, $\partial\tilde{x}/\partial\{a\}$, $\partial\dot{\tilde{x}}/\partial\{a\}$ may be analytically evaluated directly in the frequency domain from Eq. (4) and Eq. (6), only $\partial\tilde{A}/\partial\{a\}$ should be numerically evaluated by transformation to the time domain and with a difference quotient approximation. For the given $\{a^{(k)}\}$ and increment $\Delta\{a^{(k)}\}$, the corresponding $\tilde{A}^{(k)}$ and $\Delta\tilde{A}^{(k)}$ can be acquired by the numerical search within a period after $\{a^{(k)}\}$ and $\{a^{(k)}\}+\Delta\{a^{(k)}\}$ have been transformed to time domain discrete values by the inverse FFT. Thereby the finite-difference approximation of $\partial\tilde{A}/\partial\{a\}$ can be calculated.

3. Response Features of the Hysteretic Model

The proposed method can analyze the periodic forced vibrations of the hysteretic system. Here, the response features of the hysteretic model are identified by the evaluation of the frequency-response curves. Fig. 1 illustrates the frequency-response curves of the hysteretic system under harmonic excitation $F = F_0\cos\omega t$. Here $m = 1.0$ kg, $k = 0.0$, $c = 0.0$, and the hysteretic model parameters given in Ref. [1] are adopted. It is seen from Fig. 1 that the hysteretic model exhibits typical softening nonlinear responses according to the hysteresis loop characteristics [1].

The primary-harmonic components and third order harmonic components of the response are shown in Figs. 2(a) and 2(b) respectively. Since the hysteretic model is symmetrical about the origin, only odd-harmonic components are exhibited under harmonic excitation. The superharmonic responses are contributed due to the nonlinearity. In some situations, a nonlinear hysteretic system may exhibit superharmonic resonances and even subharmonic resonances [15].

Fig. 3 illustrates a numerical example of the hysteretic system subjected to multi-harmonic excitations. Here the external force with multi-exciting frequencies is taken as

$$F(t)=F_0\cdot(\cos\omega t+0.4\cdot\sin 3\omega t) \tag{13}$$

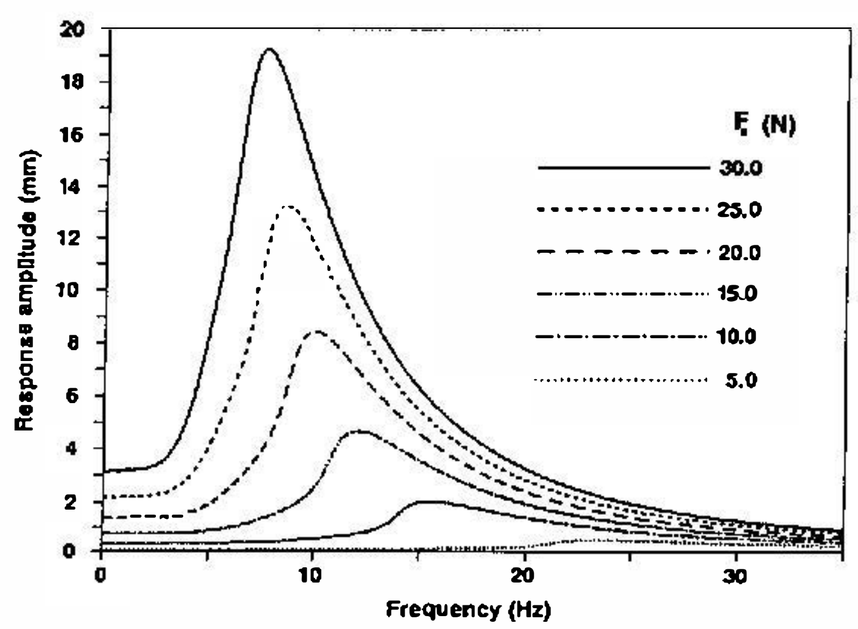

Fig. 1 Frequency-response curves of the hysteretic model

4. Analysis of Base-Isolated Structures and Experimental Verification

In recent years, the base-isolation techniques have been widely used for aseismic design [16] and for isolating the vibration from other ground excitations [17]. Some base-isolation systems have been developed; among them are nonlinear hysteretic systems [18-21]. Besides numerical integration procedures [20,21], the dynamic responses of hysteretic base-isolated structures are usually evaluated by assuming that the structures vibrate in the first mode [18,19]. Here, accurate multi-harmonic steady-state responses of hysteretic base-isolated frame structures considering higher-order modes are analyzed by the proposed method with the use of modal partial decoupling. The introduction and partial decoupling of the modal coordinates will make the computational scheme as convenient as the SDOF hysteretic system.

(a) Analysis of Base-Isolated Frame Structure

For a general elastic frame structure as shown in Fig. 4, the governing equation of motion of the system subjected to the ground excitation, can be expressed as

$$[M]\cdot\{x\}'' + [c]\cdot\{x\}' + [K]\cdot\{x\} = -[M]\cdot\{1\}\cdot x_g''(t) \tag{14}$$

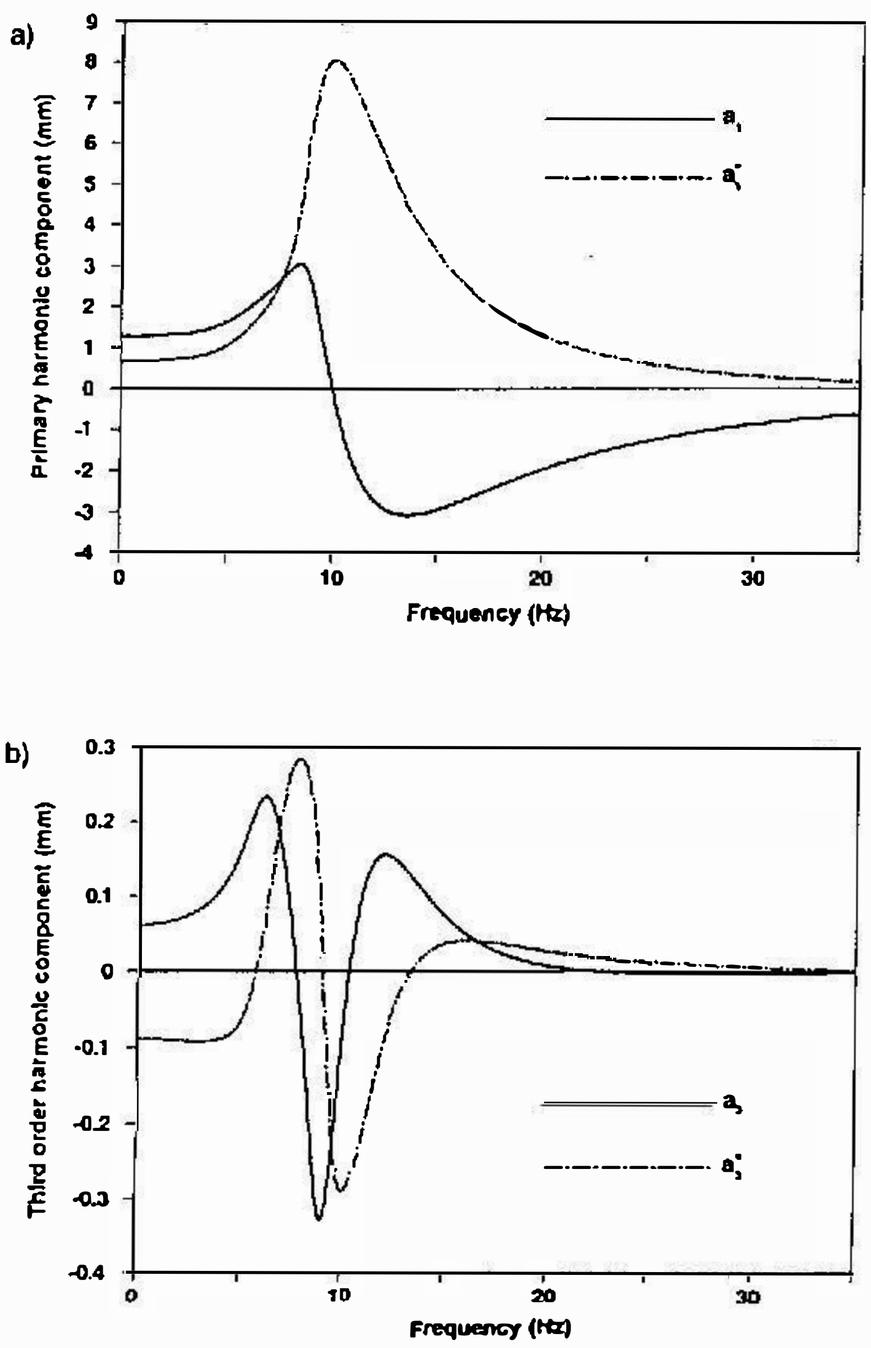

Fig. 2 Harmonic components of displacement response

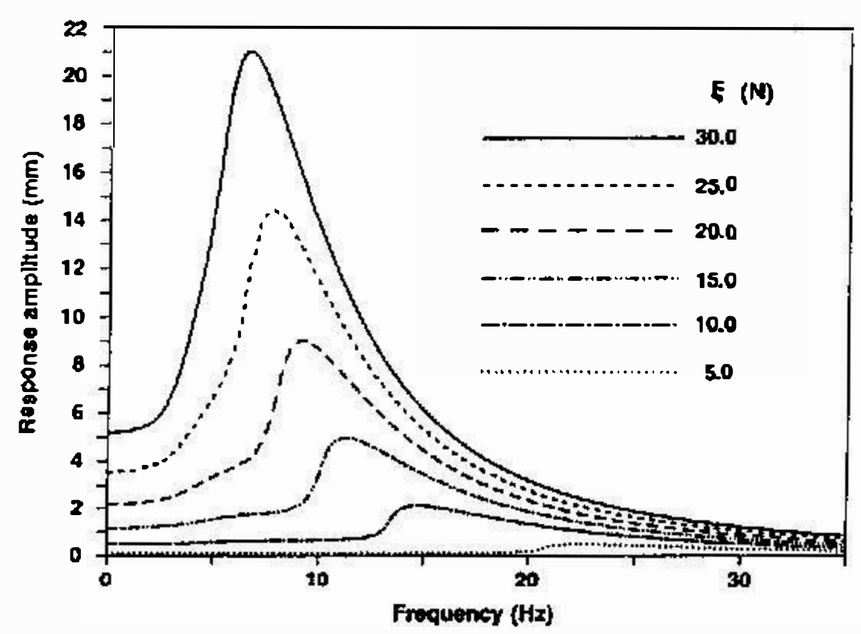

Fig. 3 Response amplitude versus frequency under multi-harmonic excitations

where $' = \frac{d}{dt}$, and [M], [C], [K] are the mass, damping and stiffness matrices of structure. $x_g''(t)$ is the ground acceleration, $\{1\}$ is a unit vector, $\{x\} = \{x_1 x_2 \mathrm{L}\ x_m\}^T$ is the vector of floor displacements relative to ground, and $\{x\}'$ and $\{x\}''$ are the relative velocity and acceleration vectors, respectively. The damping matrix [C] is assumed to be linearly dependent on both the mass and stiffness matrices and has the form

$$[c] = \alpha \cdot [M] + \beta \cdot [k] \tag{15}$$

where α and β are proportionality constants. By introducing the normal-coordinate transformation

$$\{x\} = \left[\{u_1\}\{u_2\}\mathrm{L}\ \{u_m\}\right] \cdot \{y\} = [U] \cdot \{y\} \tag{16}$$

and using the modal orthogonality, Eq. (14) can be decoupled as

$$y_j'' + 2\omega_j \xi_j y' + \omega_j^2 y_j = p_j \cdot x_g''(t) \qquad (j = 1,2,\mathrm{L}\ ,M) \tag{17a}$$

$$x_i = \sum_{j=1}^{M} u_j(i) \cdot y_j \qquad (i = 1,2,\mathrm{L}\ ,M) \tag{17b}$$

where ω_j and $\{u_j\}$ $(j = 1,2,\mathrm{L}\ ,M)$ are the jth natural frequency and mode shape vector, $\{y\} = \{y_1 y_2 \mathrm{L}\ y_M\}^T$ is the vector of modal coordinates, and

$$p_j = -\{u_j\}^T \cdot [M] \cdot \{1\} / \left(\{u_j\}^T \cdot [M] \cdot \{u_j\}\right) \tag{18}$$

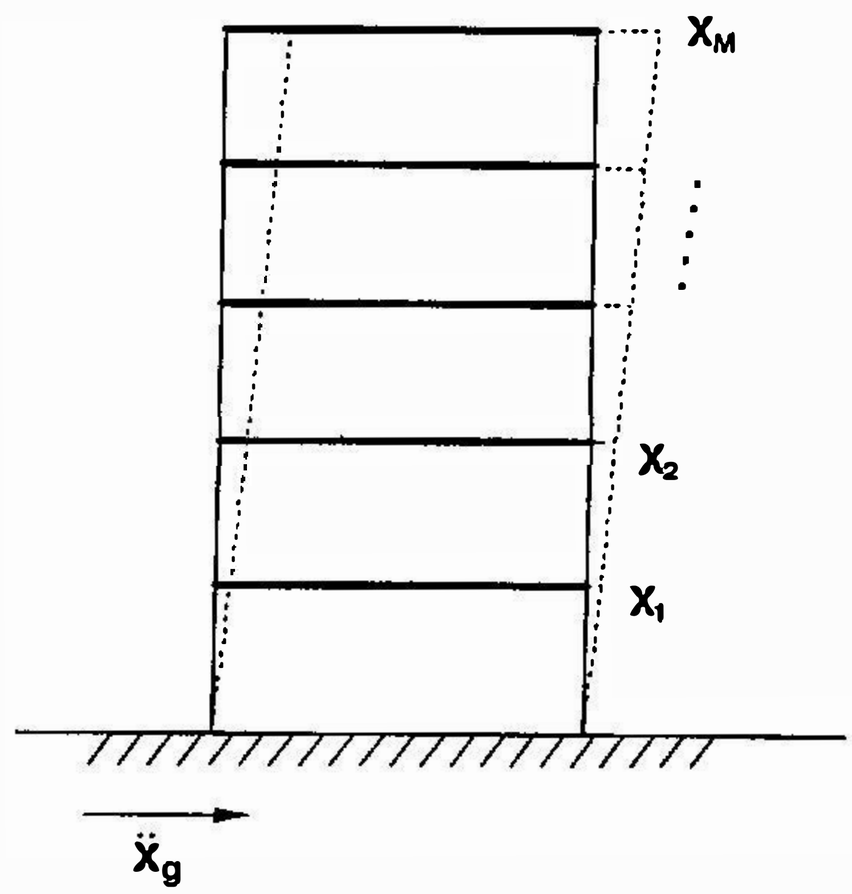

Fig. 4 Frame structure without Isolation

$$\xi_j = \frac{1}{2}\left(\beta\omega_j + \alpha / \omega_j\right) \tag{19}$$

For the structure with the base isolation illustrated in Fig. 5, the governing equations of motion of the system can be expressed as

$$[M]\cdot\{x''\}+[C]\cdot\{x'\}+[K]\cdot\{x\} = -[M]\cdot\{1\}\cdot\left(x_g'' + x_b''\right) \tag{20a}$$

$$m_b x_b'' + c_b x_b' + k_b x_b + Q(x_b, x_b', A, t) - F_1([K],\{x\}) - F_2([C],\{x'\}) = -m_b x_g'' \tag{20b}$$

where $\{x\}=\{x_1\ x_2\ \ldots\ x_M\}^T$ is the vector of floor displacements relative to the base floor, $\{x\}'$ and $\{x\}''$ are relative velocities and accelerations, m_b is the mass of the base floor, and x_b is the displacement of the base floor relative to ground. The base floor is isolated by the hysteretic isolation system having linear elastic and nonlinear hysteretic components in which k_b, c_b are the stiffness and viscous damping coefficients and $-Q(x_b, x_b', A, \omega)$ is the restoring force of the nonlinear hysteresis. The time domain amplitude of the base relative displacement x_b is given by A. $F_1([K],\{x\})$ and $F_2([C],\{x\}')$ are the linear elastic restoring force and viscous damping force acting on the base floor. $F_1([K],\{x\})$ is a known function with respect to $[K]$ and $\{x\}$ of the structure and $F_2([C],\{x\}')$, a known function with respect to $[C]$ and $\{x\}'$. For the shear structure, as a special case, $F_1([K],\{x\}) = k_1 x_1$ and $F_2([C],\{x\}') = c_1 x_1'$, where k_1, c_1 are the stiffness and viscous damping of the first floor relative to the base floor.

Suppose the natural frequencies and mode shapes of the structure (when the base floor is fixed on ground) are ω_j and $\{u_j\}$ ($j = 1, 2, \ldots, M$). By introducing the normalized coordinates, the following partially decoupled motion equations of the base-isolated structure can be achieved

$$x_i = \sum_{j=1}^{M} u_j(i)\cdot y_j \qquad (i = 1,2,\ldots,M) \tag{21a}$$

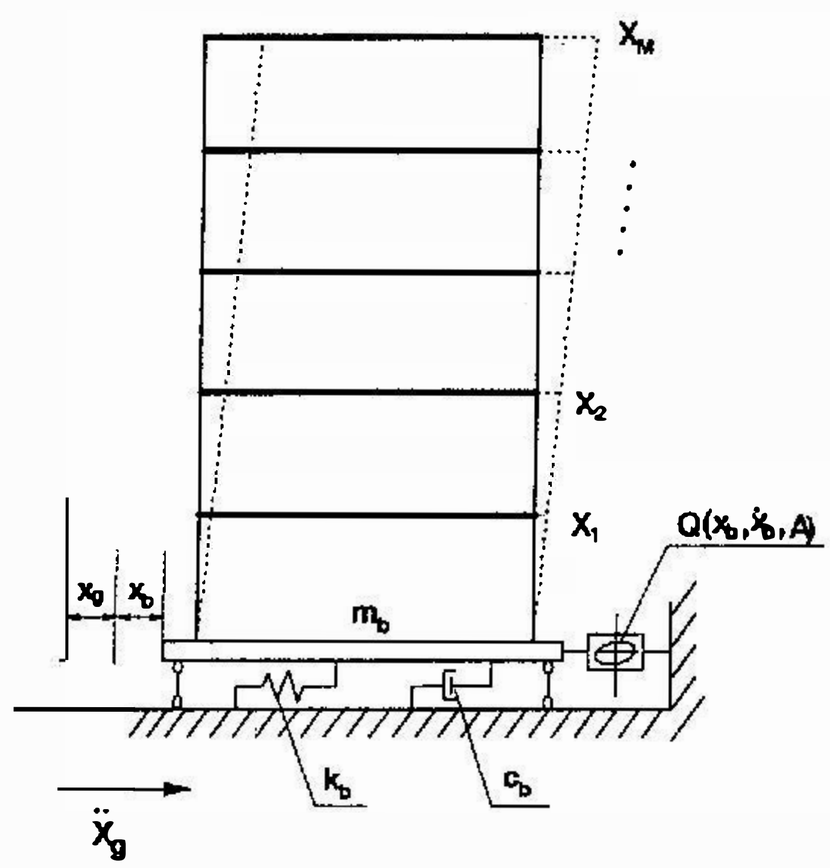

Fig. 5 Frame structure with base-isolation

$$y_j'' + 2\omega_j \xi_j y_j' + \omega_j^2 y_j = p_j \cdot \left(x_g'' + x_b''\right) \qquad (j = 1, 2, \mathrm{L}\ , M) \tag{21b}$$

$$m_b\left(x_g'' + x_b''\right) + c_b x_b' + k_b x_b + Q\left(x_b, x_b', A, t\right) - F_1\left([K], \{x\}\right) - F_2\left([C], \{x'\}\right) = 0 \tag{21c}$$

The above partially decoupled motion equations will greatly reduce the computational amount of iteration by the proposed method. In this case, only the base floor relative displacement x_b should be taken as the independent unknown, $\{y\}$ and $\{x\}$ may be regarded as auxiliary variables which can be analytically expressed in terms of a given x_b.

Equation (21c) is now referred to as the objective equation to be iterated. Applying the Galerkin method to Eq. (21c) and introducing dimensionless time $\tau = \omega t$ provides

$$k_b a_0 + m_b g_0 + q_0\left(\{a\}\right) - f_{10}\left(\{\tilde{x}\}\right) - f_{20}\left(\{\dot{\tilde{x}}\}\right) = 0 \tag{22a}$$

$$\left(k_b - m_b \omega^2 j^2\right) \cdot a_j + c_b \omega j \cdot a_j^* + m_b g_j + q_j\left(\{a\}\right) - f_{1j}\left(\{\tilde{x}\}\right) - f_{2j}\left(\{\dot{\tilde{x}}\}\right) = 0 \qquad (j = 1, 2, \mathrm{L}\ , N) \tag{22b}$$

$$-c_b \omega j \cdot a_j + \left(k_b - m_b \omega^2 j^2\right) \cdot a_j^* + m_b g_j^* + q_j^*\left(\{a\}\right) - f_{1j}^*\left(\{\tilde{x}\}\right) - f_{2j}^*\left(\{\dot{\tilde{x}}\}\right) = 0 \qquad (j = 1, 2, \mathrm{L}\ , N) \tag{22c}$$

where $\{a\} = \left\{a_0 a_1 a_2 \mathrm{L}\ a_n a_1^* a_2^* \mathrm{L}\ a_N^*\right\}^T$ is the unknown vector containing the harmonic components of the base floor relative displacement $x_b(t)$, $\{g\} = \left\{g_0\ g_1\ \mathrm{L}\ g_N\ \ g_0^*\ g_1^*\ \mathrm{L}\ g_N^*\right\}^T$ is the known vector of the harmonic components of the periodic ground acceleration $x_g''(t)$, $\{q\} = \left\{q_0\ q_1\ q_2\ \mathrm{L}\ q_N\ q_1^*\ q_2^*\ \mathrm{L}\ q_N^*\right\}^T$ is the vector of the harmonic components of $Q\left(\tilde{x}_b, \dot{\tilde{x}}, \tilde{A}, t\right)$, the vectors $\{f_1\} = \left\{f_{10}\, f_{11}\, f_{12}\, \mathrm{L}\ f_{1N}\, f_{11}^*\, f_{12}^*\, \mathrm{L}\ f_{1N}^*\right\}^T$ and $\{f_2\} = \left(f_{20}\, f_{21}\, f_{22}\, \mathrm{L}\ f_{2N}\, f_{21}^*\, f_{22}^*\, \mathrm{L}\ f_{2N}^*\right)^T$ comprises the Fourier expansion coefficients of $F_1\left([K]\{\tilde{x}\}\right)$ and $F_2\left([C]\{\dot{\tilde{x}}\}\right)$, respectively.

Compared with Eq. (10), only $\{f_1\}$ and $\{f_2\}$ in Eq. (22) are additional. When the Galerkin/Levenberg-Marquardt procedure is applied, for a given $\{a^{(k)}\}$, corresponding harmonic components of $\{\tilde{y}\}$ and $\{\tilde{x}\}$ may be explicitly expressed in terms of $\{g\}$ and $\{a^{(k)}\}$ from Eqs. (21a) and (21b). The time domain discrete values of $F_1([K],\{\tilde{x}\})$, $F_2([C],\{\dot{x}\})$, $\partial F_1([K],\{\tilde{x}\})/\partial\{a\}$ and $\partial F_2([C],\{\dot{\tilde{x}}\})/\partial\{a\}$ within a period, can be evaluated after the inverse FFT for the harmonic components of $\{\tilde{x}\}$ and $\{\dot{\tilde{x}}\}$. Thereby $\{f_1(\{\tilde{x}\})\}$, $\{f_2(\{\dot{\tilde{x}}\})\}$, $\partial\{f_1(\{\tilde{x}\})\}/\partial\{a\}$ and $\partial\{f_2(\{\dot{\tilde{x}}\})\}/\partial\{a\}$ with $\{a\}=\{a^{(k)}\}$ can be obtained by a forward FFT for these discrete sequences. For a special case, when $F_1([K],\{x\})$ and $F_2([C],\{\dot{x}\})$ are linear functions of $\{x\}$ and $\{\dot{x}\}$ respectively, $\{f_1(\{\tilde{x}\})\}$, $\{f_2(\{\dot{\tilde{x}}\})\}$, $\partial\{f_1(\{\tilde{x}\})\}/\partial\{a\}$, $\partial\{f_2(\{\dot{\tilde{x}}\})\}/\partial\{a\}$ can be directly derived from the harmonic components of $\{\tilde{x}\}$ without applying frequency/time domain alternation. After $\{f_1(\{\tilde{x}\})\}$, $\{f_2(\{\dot{\tilde{x}}\})\}$, $\partial\{f_1(\{\tilde{x}\})\}/\partial\{a\}$, and $\partial\{f_2(\{\dot{\tilde{x}}\})\}/\partial\{a\}$ are evaluated, Eq. (21c) can be solved as the SDOF hysteretic system by the proposed method and the solutions $\{a\}$ and $\{x\}$ are reached.

(b) Base-Isolation Tests

A two-story steel frame model as shown in Fig. 6, is dynamically experimented upon. The dynamic behaviors of the frame are measured by impact testing and sweep sinusoidal testing. The arrangement of the modal measurement is illustrated in Fig. 7. The natural frequencies of the frame are measured to be f_1= 9. 52 Hz and f_2= 30. 51 Hz. The measured viscous damping ratios are ξ_1= 0. 0036 and ξ_2= 0. 0010. The floor relative stiffnesses are identified to be k_1= 5. 82 N/mm and k_2=8. 87 N/mm.

A hanging shaking platform is arranged for base-isolation tests of the frame. This platform has been used for dynamic behavior testing of hysteretic isolators [1]. In this experimental setup, as shown in Fig. 8, two rigid plates are hung in parallel on a trestle through frictionless hinges connected with four rigid steel tubes to form a double-pendulum system. The lateral movement of the system is prevented with guiding rollers. For the hysteretic isolators with dry friction damping properties, the restoring forces are affected by static preloading. Thereby the shaking platform is designed as a hanging double-pendulum to eliminate vertical preloading. The pendulum length should be large enough so the vertical movement accompanying the swing can be ignored. When the horizontal displacement of the platform is x=5 mm, the additional vertical displacement x_v is equal to 0. 025 mm which is much less than x.

The schematic diagram of the base-isolation tests is illustrated in Fig. 9. The frame is fixed on the upper plate. Two JGS-1 wire-cable vibration isolators are mounted and fixed with their aluminum retainer bars to the upper and lower plates. The base floor mass $m_b=m_0+m_p$=10. 2kg, where m_p is the mass of the upper

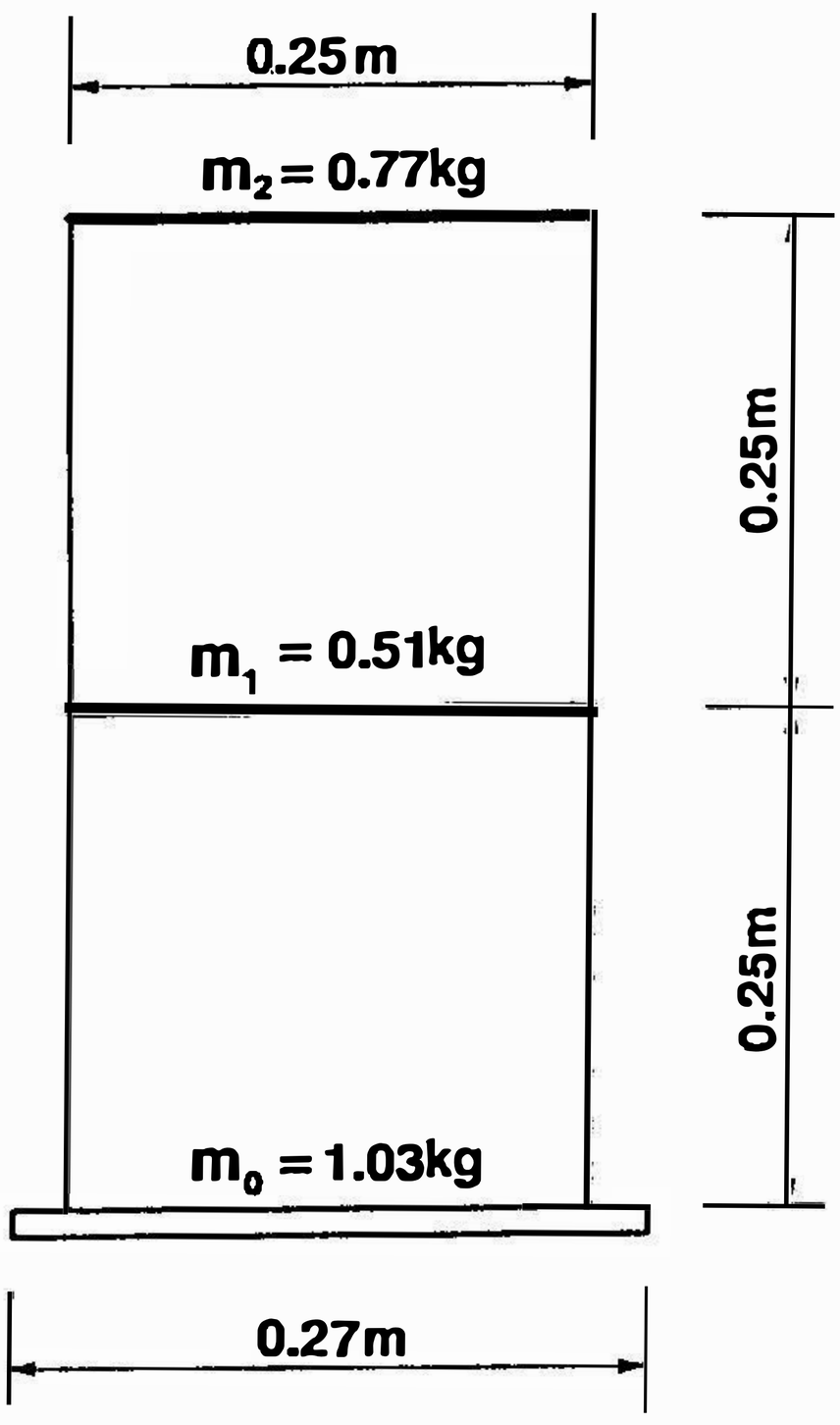

Fig. 6 A two-story frame model

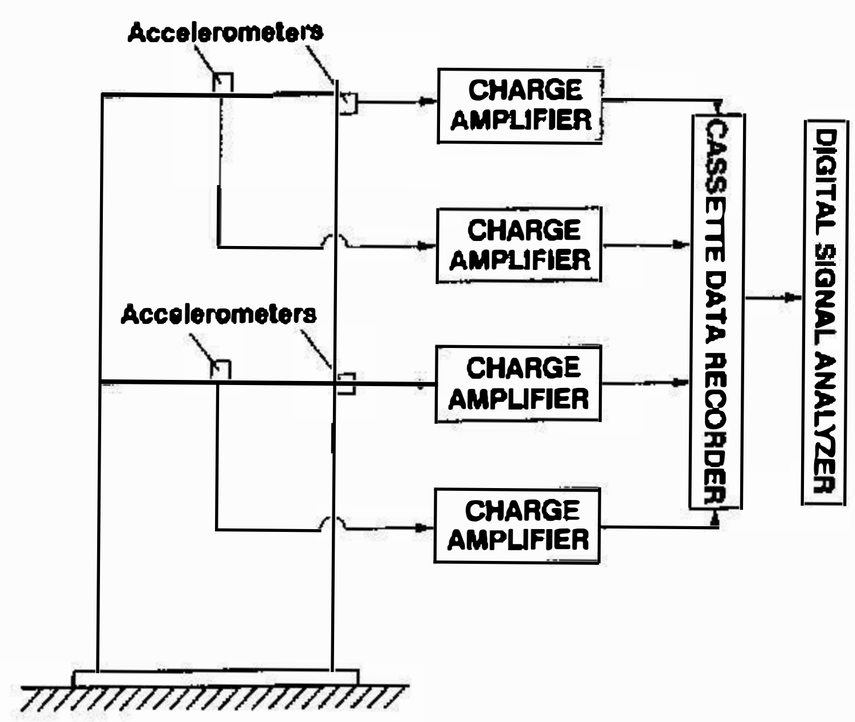

Fig. 7 Modal measurement of tested frame

pendulum and $k_b = c_b = 0$. The lower plate is horizontally excited to simulate the ground vibration. The experiments are executed by the frequency sweep with constant-amplitude and by the discrete-frequency harmonic excitation. Fig. 10 shows a measured frequency-response curve of the base-isolated frame recorded by the graphic level recorder.

(c) Comparison of Analytical and Experimental Responses

The analytical responses of the tested frame before and after base-isolation are evaluated by the proposed method and are compared with the experimental findings. Fig. 11 shows the frequency-response curve of the unisolated frame subjected to ground acceleration $x_g''(t) = A_g \cos \omega t$. Here A_2/A_g is the ratio of the acceleration response amplitude of the top floor to the ground acceleration. The solid line denotes the analytical response curve and the scattered points are the experimental results under the discrete-frequency harmonic excitation.

Figs. 12 (a-d) illustrate the frequency-response curves of the base-isolated frame, respectively, with the

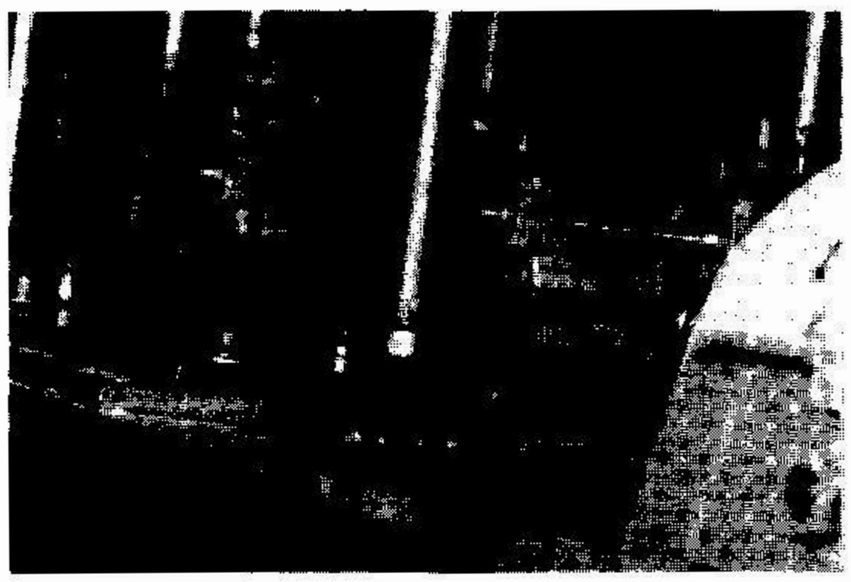

Fig. 8 Setup of hanging shaking platform

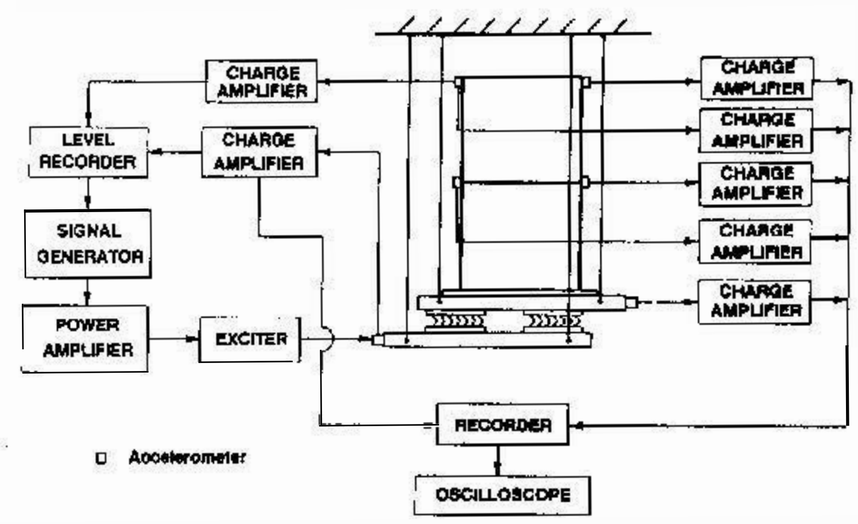

Fig. 9 Schematic diagram of base-isolation tests

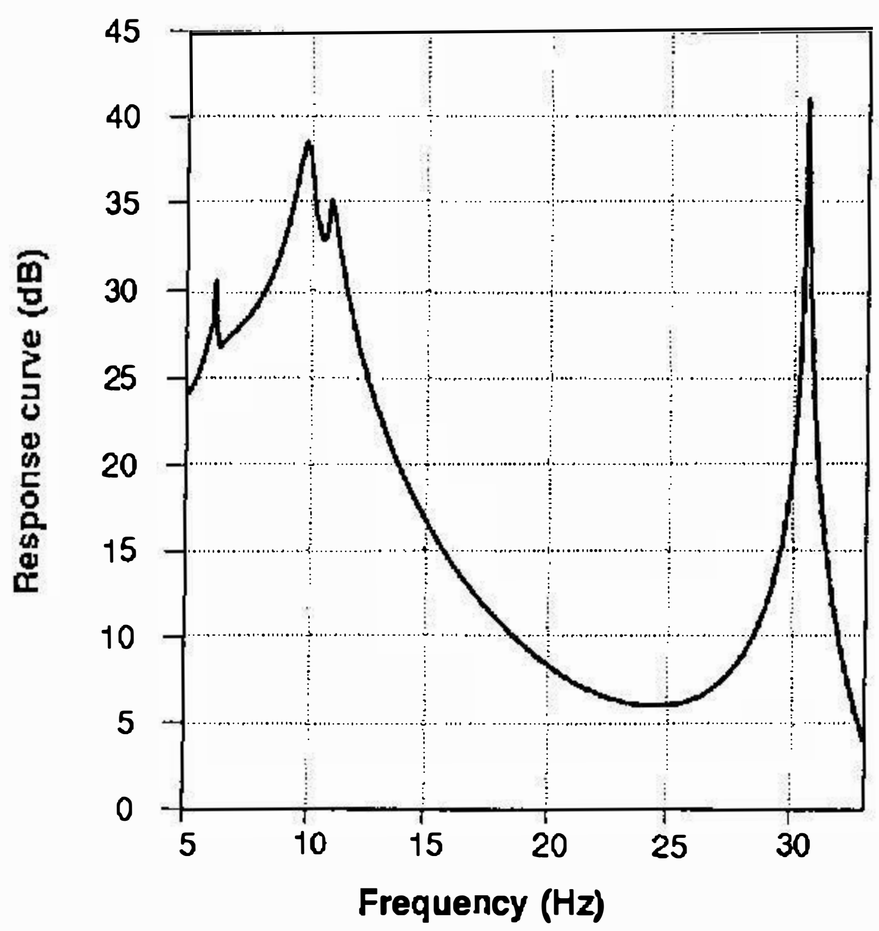

Fig. 10 Measured frequency-response curve of isolated frame

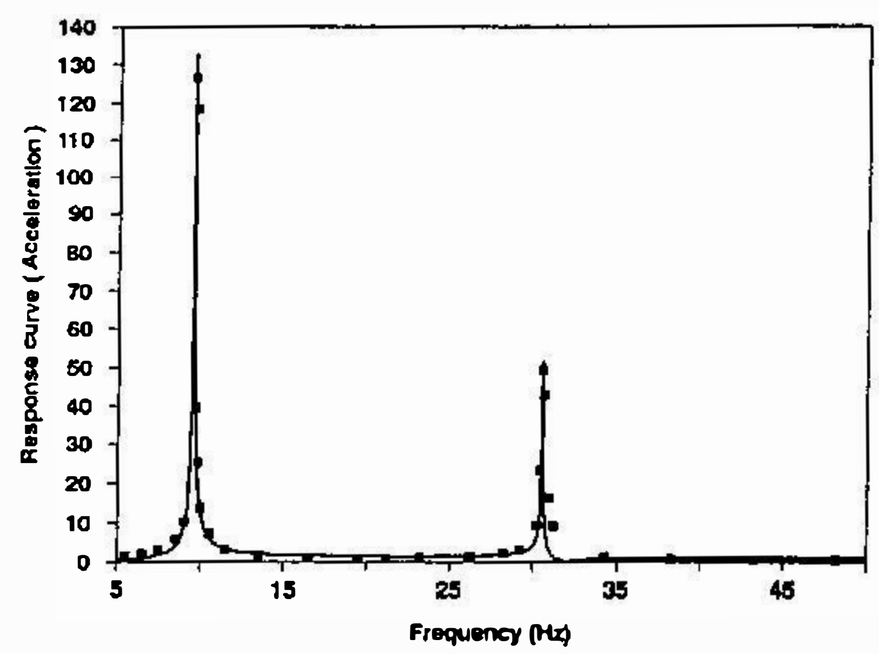

Fig. 11 Frequency-response curve A_2/A_g before isolation

excitation amplitude A_g=0.6 m/s^2, 1.4 m/s^2, 2.3 m/s^2 and 3.2 m/s^2. Solid lines show the computational response curves and the scattered points are experimental results.

The frequency-response curve of the unisolated frame exhibits two peaks, corresponding to two natural frequencies. It is seen from Figs. 10 and 12 that, after base-isolation, both the analytical and experimental frequency-response curves of this 3 DOF system exhibit more than three response peaks due to nonlincarity. Fig. 13 illustrates the primary- and super-harmonic components of the top floor acceleration response x_2'' and Fig. 14 shows the response curves of the base floor relative displacement x_b. It is clearly seen that, at the frequencies of approximately 9.8 Hz and 30.5 Hz, the cosine and sine primary-harmonic components simultaneously reach peaks and the base floor relative displacement response approaches zero regardless of excitation amplitude. So the resonant peaks corresponding to these two frequencies in Fig. 12 are caused by the natural frequencies of the frame and other response peaks, for which the frequency locations vary with the excitation amplitude, are contributed from the nonlinear stiffness of hysteretic isolators.

It is seen from Fig. 14(a) that, since the nonlinear stiffness of the hysteretic isolators depends on the response behavior, the response curve of the base floor relative displacement exhibits some resonant peaks in the different frequency ranges. The frequency of every peak decreases with the increase of excitation amplitude conforming to the softening feature of the hysteretic isolators. Correspondingly, in Figs. 12(a-d), the peaks of the top floor acceleration response curve, except those pertinent to the two natural frequencies of the frame, have descending frequencies with the increase of the excitation amplitude. It is

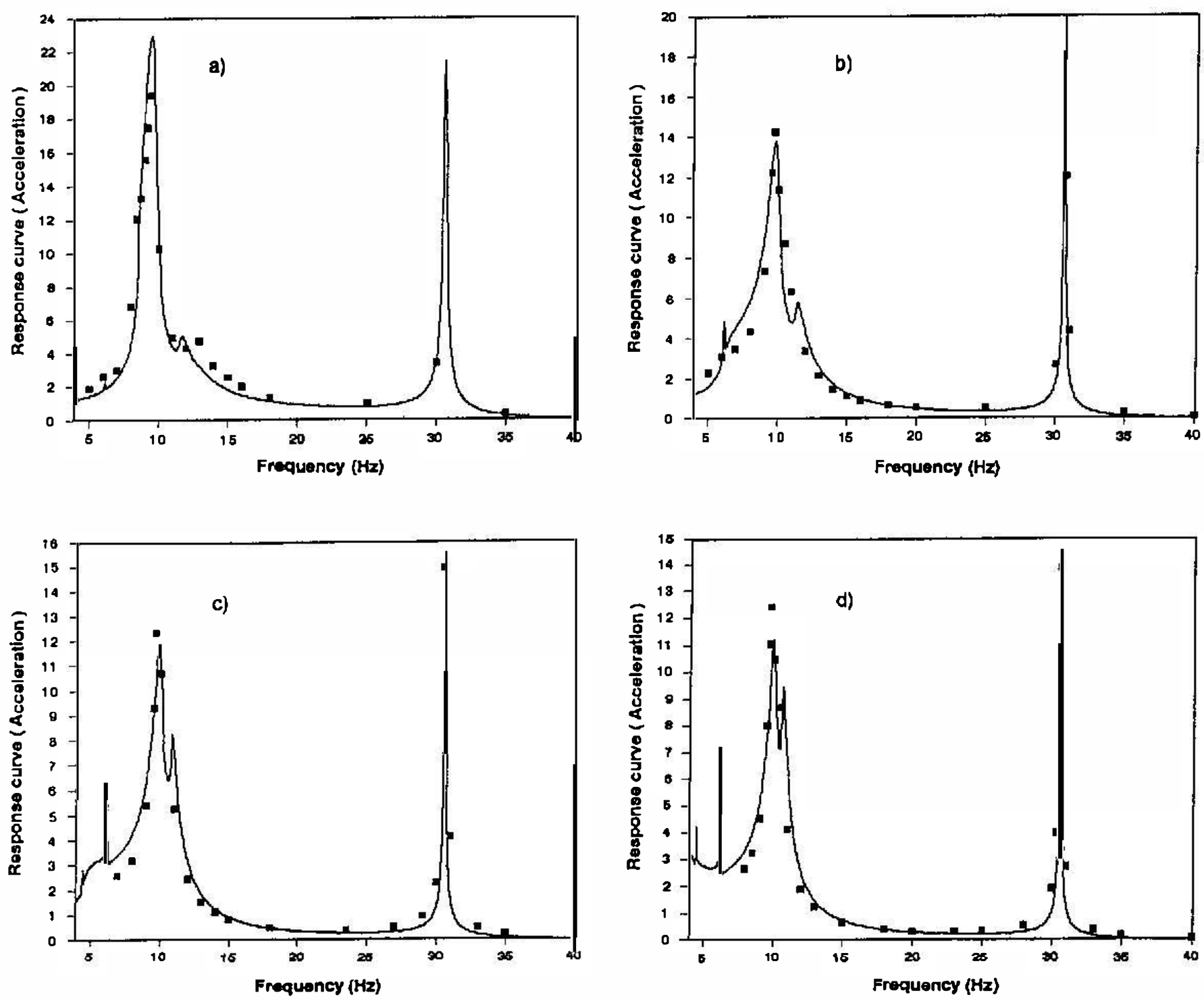

Fig. 12 Frequency-response curve A_2/A_g, after base-isolation.

observed from Figs. 13(a-b) that, besides primary-harmonic resonances, *superharmonic* resonances also occur in different frequency locations due to the nonlinearity. The values of the superharmonic components rise with the increase of excitation magnitude. Therefore, in the case of large excitation, many response peaks may occur in the low frequency range owing to superharmonic resonances. In addition, in some situations, nonlinear hysteretic systems may exhibit multi-valued frequency-response curves [15].

5. Concluding Remarks

A method for analyzing the periodic forced vibration of structures with nonlinear hysteretic isolators is presented and the computer program is developed. The proposed method can evaluate multi-harmonic dynamic responses of hysteretically isolated structures including superharmonic resonances.

A two-story frame model, isolated at its base by wire-cable isolators, is dynamically experimented upon and the analytical responses of this structure are computed by the proposed method. Good agreement between the analytical responses and the experimental findings was observed. It is found from the analytical and experimental results that the frequency-response curve of the base-isolated structure exhibits more resonant peaks than the DOF number due to hysteretic nonlinearity. Under simple harmonic excitation, the hysteretic structure contributes multi-harmonic responses. The frequency-response curve may exhibit many resonant peaks in the low frequency range owing to superharmonic resonances, especially in the case of large excitation.

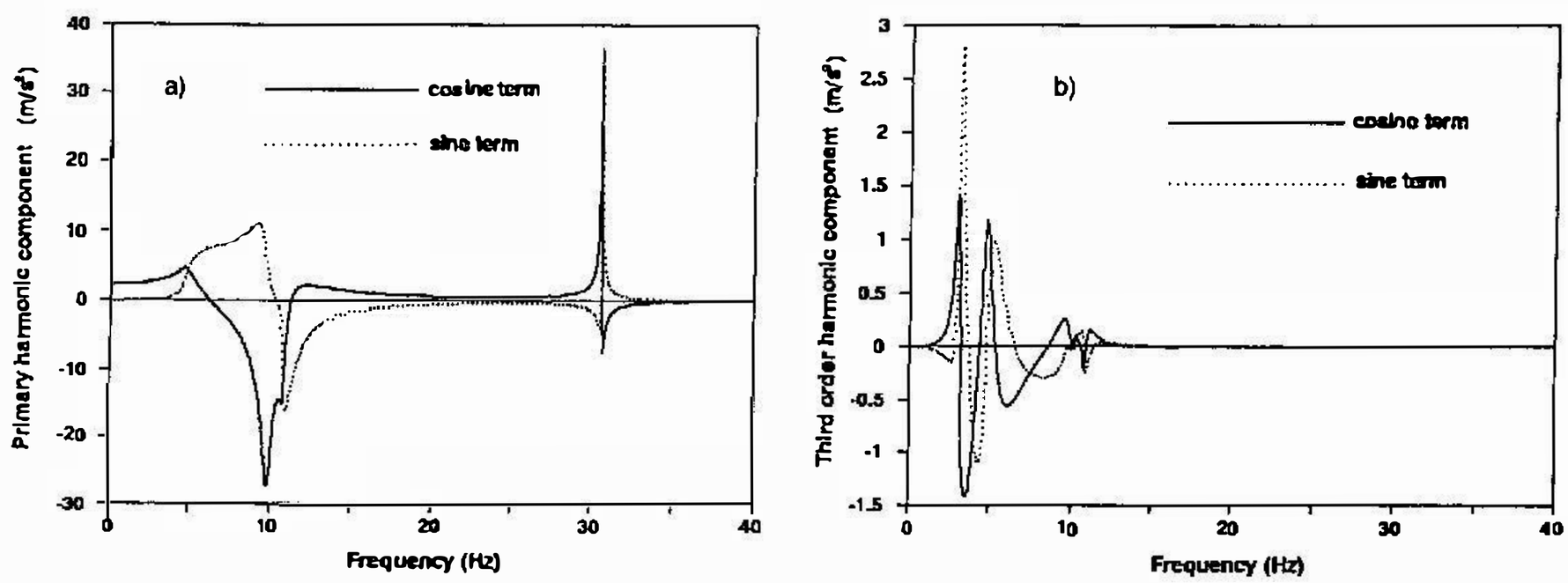

Fig. 13 Harmonic components of top floor acceleration response

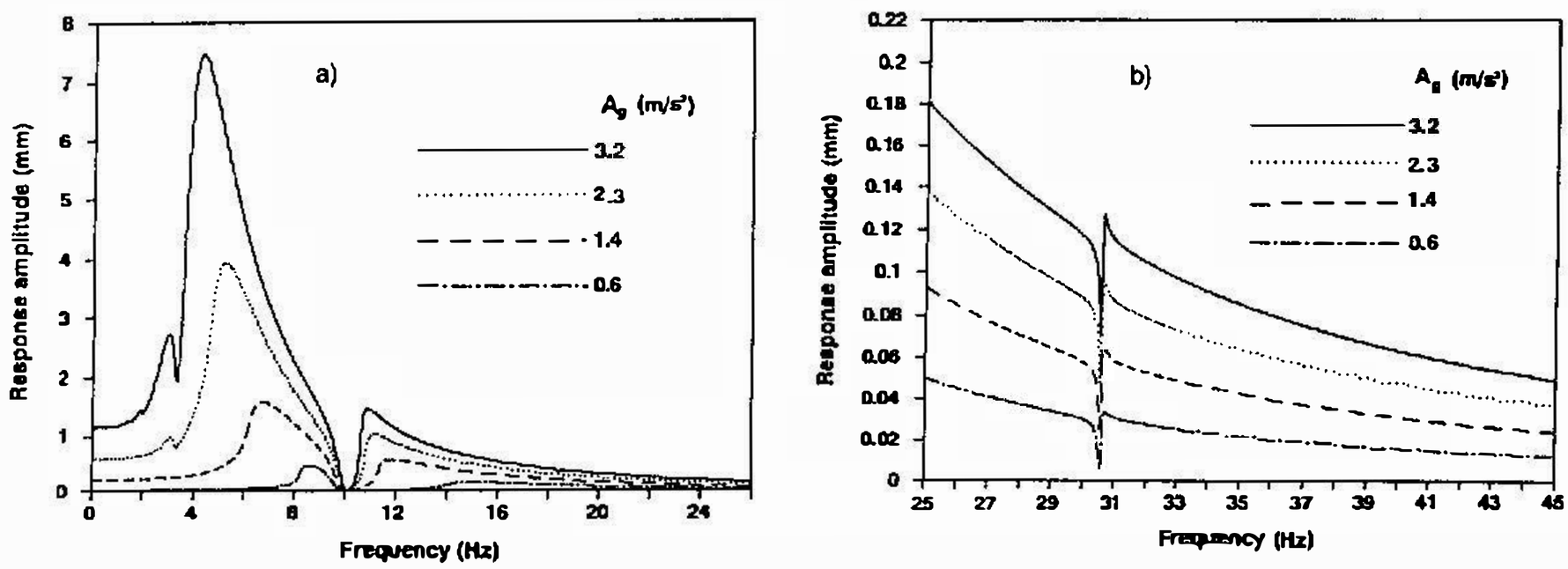

Fig. 14 Response curves of base floor relative displacement

Acknowledgements

The financial support by the U.P.G.C. Earmarked Grant of Hong Kong Government is gratefully acknowledged. The authors also wish express their thanks to Mr. M.C. Ng and Mr. J.Y.H. Lam for the design of experimental apparatus.

References

[1] Ko, J.M.; Ni, Y.Q.; Tian, Q.L. "Hysteretic Behavior and Empirical Modeling of a Wire-Cable Vibration Isolator." *Int J Anal Exp Modal Anal* v 7 n 2 Apr 1992 p 111-127.

[2] Lau, S.L.; Cheung, Y.K. "Amplitude Incremental Variational Principle for Nonlinear Vibration of Elastic Systems." *J Appl Mech Trans ASME* v 48 n 4 1981 p 959-964.

[3] Cheung, Y.K.; Lau, S.L. "Incremental Time-Space Finite Strip Method for Non-linear Structural Vibrations." *Earthquake Eng Struct Dyn* v 10 n 2 1982 p 239-253.

[4] Lau, S.L.; Cheung, Y.K.; Wu, S.Y. "Incremental Harmonic Balance Method with Multiple Time Scales for Aperiodic Vibration of Nonlinear Systems." *J Appl Mech Trans ASME* v 50 n 3 1983 p 871-876.

[5] Pierre, C.; Ferri, A.A.; Dowell, E.H. "Multi-harmonic Analysis of Dry Friction Damped Systems Using an Incremental Harmonic Balance Method." *J Appl Mech Trans ASME* v 52 n 4 1985 p 958-964.

[6] Cheung, Y.K.; Chen, S.H.; Lau, S.L. "Application of the Incremental Harmonic Balance Method to Cubic Non-linearity Systems." *J Sound Vib* v 140 n 2 1990 p 273-286.

[7] Wong, C.W.; Zhang, W.S.; Lau, S.L. "Periodic Forced Vibration of Unsymmetrical Piecewise-linear Systems by Incremental Harmonic Balance Method." *J Sound Vib* v 149 n 1 1991 p 91-105.

[8] Tamura, H.; Tsuda, Y.; Sueoka, A. "Higher Approximation of Steady Oscillations in Nonlinear Systems with Single Degree of Freedom (Suggested Multi-Harmonic Balance Method)." *Bull JSME* v 24 n 195 1981 p 1616-1625.

[9] Ferri, A.A.; Dowell, E.H. "Frequency Domain Solutions to Multi-degree of Freedom, Dry Friction Damped Systems." *J Sound Vib* v 124 n 2 1988 p 207-224.

[10] Wei, S.-T.; Pierre, C. "Effects of Dry Friction Damping on the Occurrence of Localized Forced Vibrations in Nearly Cyclic Structures." *J Sound Vib* v 129 n 3 1987 p 397-416.

[11] Ling, F.H.; Wu, X.X. "Fast Galerkin Method and its Application to Determine Periodic Solutions of Nonlinear Oscillators." *Int J Non Linear Mech* v 22 n 2 1987 p 89-98.

[12] Cameron, T.M.; Griffin, J.H. "An Alternating Frequency/Time Domain Method for Calculating the Steady-state Response of Nonlinear Dynamic Systems." *J Appl Mech Trans ASME* v 56 n 1 1989 p 149-154.

[13] Badrakhan, F. "Rational Study of Hysteretic Systems Under Stationary Random Excitation." *Int J Non Linear Mech* v 22 n 4 1987 p 315-325.

[14] Badrakhan, F. "Dynamic Analysis of Yielding and Hysteretic System by Polynomial Approximation." *J Sound Vib* v 125 n 1 1988 p 23-42.

[15] Wong, C.W.; Ni, Y.Q.; Lau, S.L. "Steady-state Oscillation of the Hysteretic Differential Model." Submitted to *J Eng Mech*

[16] Kelly, J.M. "A Seismic Base Isolation: Review and Bibliography." *Soil Dyn Earthquake Eng* v 5 n 4 1986 p 202-216.

[17] Newland, D.E.; Hunt, H.E.M. "Isolation of Buildings from Ground Vibration: A Review of Recent Progress." *J Mech Eng Sci* v 205 n 1 1991 p 39-52.

[18] Constantinou, M.C.; Tadjbakhsh, I.G. "Hysteretic Dampers in Base Isolation: Random Approach." *J Struct Eng* v 111 n 4 1985 p 705-721.

[19] Li, X.M. "Optimization of the Stochastic Response of a Bridge Isolation System with Hysteretic Dampers." *Earthquake Eng Struct Dyn* v 18 n 7 1989 p 951-964.

[20] Fujita, T.; Sasaki, Y.; Fujimoto, S.; Tsuruya, C. "Seismic Isolation of Industrial Facilities Using Lead-Rubber Bearing." *JSME Int J Ser 3* v 33 n 3 1990 p 427-434.

[21] Fan, F.-G.;Ahmadi, G.;Tadjbakhsh, I.G. "Multi-story Base-isolated Buildings Under a Harmonic Ground Motion." *Nucl Eng Des* v 123 n 1 1990 pp 1-26.